IMECE2014-37492

STRUCTURAL INTEGRITY OF CONVENTIONAL AND MODIFIED RAILROAD BEARING ADAPTERS FOR ONBOARD MONITORING

Joseph Montalvo
Mechanical Engineering Department
The University of Texas-Pan American
1201 W. University Dr., Edinburg, TX 78539,
email: **jmmontalvo@broncs.utpa.edu**

Alexis Trevino
Mechanical Engineering Department
The University of Texas-Pan American
1201 W. University Dr., Edinburg, TX 78539,
email: **atrevinow@broncs.utpa.edu**

Arturo A. Fuentes, Ph.D.
Mechanical Engineering Department
The University of Texas-Pan American
1201 W. University Dr., Edinburg, TX 78539,
Tel: (956) 665-7099; Fax: (956) 665-3527,
email: **aafuentes@utpa.edu**

Constantine M. Tarawneh, Ph.D.
Mechanical Engineering Department
The University of Texas-Pan American
1201 W. University Dr., Edinburg, TX 78539,
Tel: (956) 665-2607; Fax: (956) 665-3527,
email: **tarawneh@utpa.edu**

ABSTRACT

This paper presents a detailed study of the structural integrity of conventional and modified railroad bearing adapters for onboard monitoring applications. Freight railcars rely heavily on weigh bridges and stations to determine cargo load. As a consequence, most load measurements are limited to certain physical railroad locations. This limitation provided an opportunity for an optimized sensor that could potentially deliver significant insight on bearing condition monitoring as well as load information. Bearing adapter modifications (e.g. cut-outs) were necessary to house the sensor and, thus, it is imperative to determine the reliability of the modified railroad bearing adapter, which will be used for onboard health monitoring applications. To this end, this study quantifies the impact of the proposed modifications on the adapter structural integrity through a series of experiments and finite element analyses. The commercial software Algor 20.3TM is used to conduct the stress finite element analyses. Different loading scenarios are simulated with the purpose of obtaining the conventional and modified bearing adapter stresses during normal and abnormal operating conditions. This information is then used to estimate the lifetime of these bearing adapters. Furthermore, this paper presents an experimentally validated finite element model which can be used to attain stress distribution maps of these bearing adapters in different service conditions. The maps are also useful for identifying areas of interest for an eventual inspection of conventional or modified railroad bearing adapters in the field.

INTRODUCTION

The railroad bearing adapter act as a medium between the axle assembly (bearing, wheels) and the side frame. Figure 1 below shows the railcar truck assembly. The full-load experienced by a typical railcar in the US is 286,000 lbf, and there are a total of eight bearings on four axles supporting the railcar. This correlates to a distributed load of 35,750 lbf per bearing or bearing adapter. In order to increase the railway reliability, the University of Texas-Pan American Railroad Research Group has been working on a sensor for bearing health monitoring including load information.
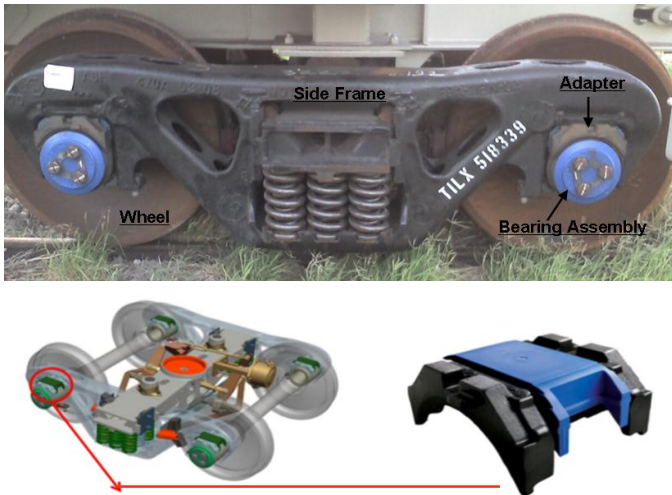
Figure 1: Railcar Truck Assembly and Railroad Bearing AdapterPlus™ with Elastomer Pad-Liner [Schematics are Courtesy of Amsted Rail[*]]

Figure 2: Original Railroad Bearing AdapterPlus™ without Elastomer Pad-Liner

Figure 3: Modified Railroad Bearing AdapterPlus™ for Onboard Monitoring without Elastomer Pad-Liner

Currently, railroad industry relies heavily on weigh bridges and stations to determine cargo load. As a consequence, most load measurements are limited to certain physical railroad locations. In a similar way, the railroad industry employs other monitoring equipment to warn of impending bearing failures. In this case, the conventional method is to place wayside hot-box detectors (HBDs) at strategic intervals to record bearing cup temperatures as the train passes at specified velocities. HBDs take a snapshot of the bearing temperature at designated wayside detection sites which may be spaced as far apart as 65 km (~40 mi) [1]. The discrete nature and limited accuracy of current weigh bridges and stations and HBDs prevent them from being utilized as a true continuous load and bearing health monitoring system. This limitation provided an opportunity for an optimized sensor that could potentially deliver significant insight on bearing condition monitoring as well as load information.

Future technologies are focusing on more frequent weight and temperature tracking of loads and bearings. Since placing sensors directly on the bearing cup is not feasible due to cup indexing during service, the next logical location for such sensors is the bearing adapter. However, bearing adapter modifications (e.g. cut-outs) were necessary to house the sensor. The insert is embedded in the bearing adapter between the Adapter Plus™ Pad and the railroad bearing. Original railroad bearing adapters have gone through modification to house the insert. The modifications to the railroad bearing adaptors include the removal of material to accommodate the insert. Figures 2 and 3 show the contrast between the non-modified and modified bearing adapters without an elastomer pad-liner and an insert.
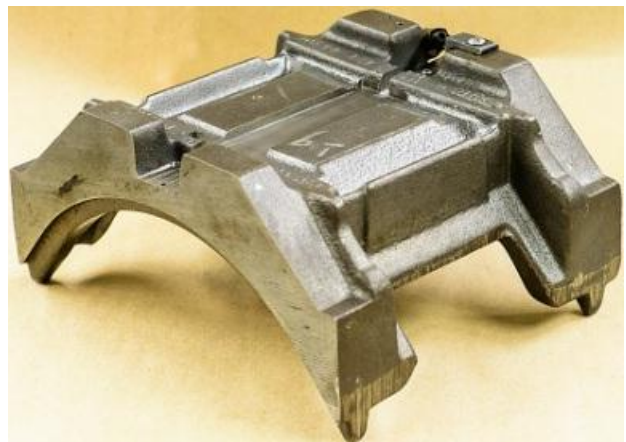
The purpose of this work is to study the structural integrity of the modified railroad bearing adapters to ensure survivability throughout operation. It is imperative to determine the reliability of the modified railroad bearing adapter, which will be used for onboard health monitoring applications. To this end, this study quantifies the impact of the proposed modifications on the adapter structural integrity. For full understanding and verification of the structural integrity, a finite element model was developed to replicate the loading (Figure 4) from the bearing cup and the adapter pad to the adapter. This paper describes the experimentally validated finite element analyses conducted for the understanding of the structural integrity of bearing adapters during operation. Assuming full static loads, several boundary conditions were tested. Initially, the raceways of the bearing adapter were fully supported in the interface with the bearing cup while a uniform distributed pressure was applied in the interface with the pad-liner (ideal loading conditions on the adapter). In

---

[*] www.amstedrail.com

addition to this scenario, based on laboratory experiments, the overall arc of support along the raceways was decreased to investigate the effects of only partially supporting the raceways in the interface with the bearing cup. Finally, also based on laboratory experiments, the effect of a non-uniform distributed pressure in the pad-liner interface was studied.
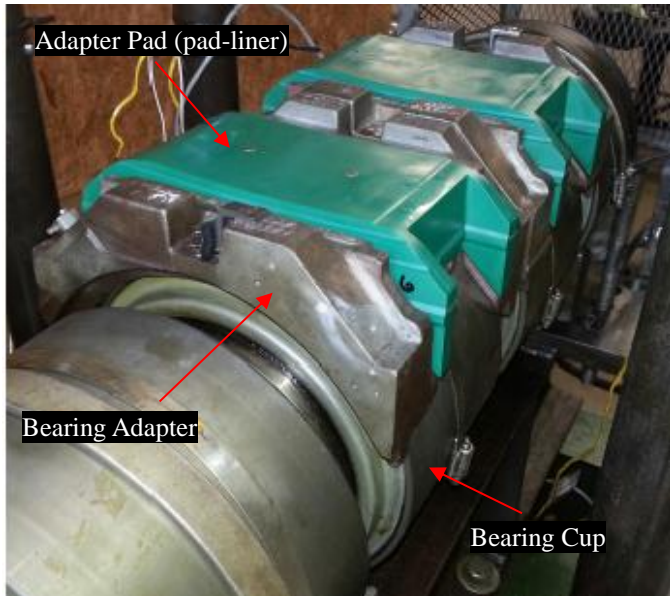

Figure 4: Railroad Bearing Cup, Adapter and Pad

LITERATURE REVIEW

In order to increase understanding and reduce time and cost, many researchers have utilized Finite Element Analysis (FEA) to study specific phenomena in different types of bearing assemblies [2-5]. It is usually recommended that the FEA studies be presented with experimentally acquired data that corroborates the validity of the proposed boundary conditions and the accuracy of the devised Finite Element (FE) models (e.g. to validate loads, boundary conditions, material and interface properties, and/or ambient conditions).

Initial studies of the structural integrity of bearing adapters for onboard monitoring were conducted by Lorenzo Saenz IV [6] at the University of Texas-Pan American (UTPA). Recently, laboratory experiments and additional Finite Element Analyses were conducted to refine and validate the initial work. The data obtained from laboratory testing was used to validate the FE model presented here. The FE method was utilized to gain a better understanding of the structural integrity of bearing adapters during operation.

EXPERIMENTAL STUDIES

Initial analysis involved finding the appropriate boundary conditions required to obtain accurate results during normal operating conditions. The laboratory experiments described in this section, conducted at UTPA, were performed using the class K bearing adapter with elastomer pad-liner. The class K bearing adapter is composed of Iron-Ductile 60-14-18. The elastomer pad-liner had similar properties to that of the TPU Elastollan 1154 D10 [6].

Pressure loads between the bearing cup and the adapter and between the elastomer pad-liner and the adapter can significantly affect the load distribution transferred to the bearing adapter. Consequently, this load distribution can dictate the final integrity of the bearing adapter. Values for the contact pressure between the bearing cup and the adapter and between the elastomer pad-liner and the adapter were obtained for the AdapterPlus™ class K based on pressure film experiments. The pressure film test has a limit in the amount of pressure it can accurately detect. Two ranges of pressure film were utilized, one having a range of 300-1,400 psi, and one with a range of 300-1,565 psi.

Figures 5 and 6 show the results of the pressure film tests (i.e. the load pattern and contact pressure) at full load (~35,750 lbf) between the bearing cup and the adapter [7]. These pressure film experiments show that the bearing AdapterPlus™ has an evenly distributed load pattern for approximately 4 inches of the arc length of the bearing adapter. A maximum contact pressure of approximately 10,032 kPa (1455 psi) is present in the pressure test. The change of overall arc of support along the raceways could be explained by variations in the manufactured parts which would affect specific surface interactions between the bearing cup and adapter (i.e., surface finish, radius of curvature, etc.). After the study of the bearing cup and adapter interface, the interface between the elastomer pad-liner and the bearing adapter was examined.
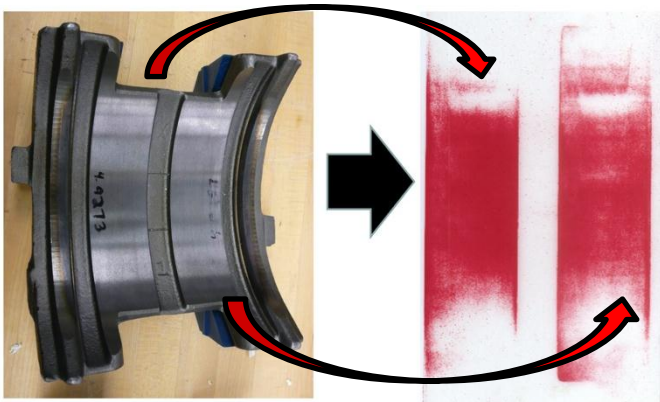
Figure 5: Load Pattern between the Bearing Cup and the Bearing AdapterPlus™ (Bottom view of Class K Bearing Adapter)
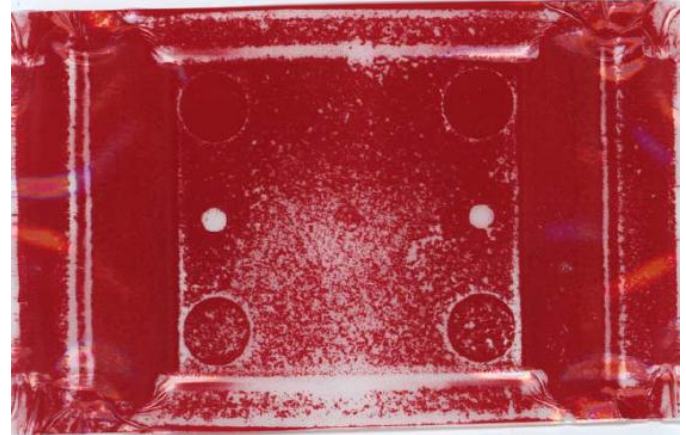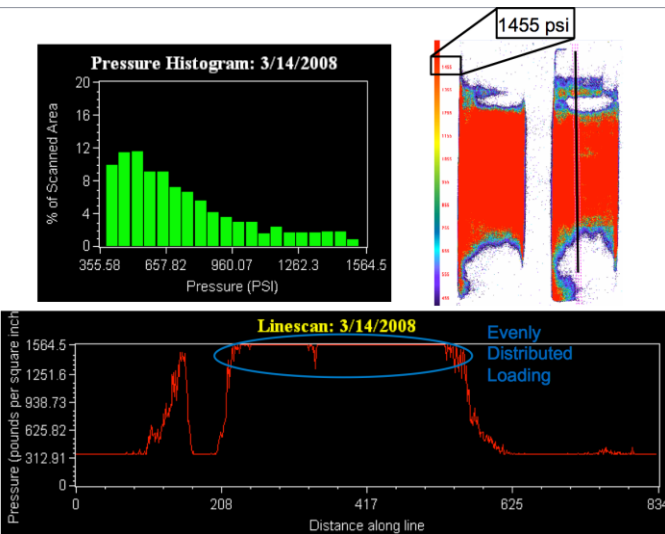

Figure 6: Load Pattern Analysis for Bearing AdapterPlus™

Figures 7 and 8 show the results of the pressure film tests for the load pattern and contact pressure at full load (~35,750 lbf) between the elastomer pad-liner and the bearing adapter. These pressure film experiments show that the bearing AdapterPlus™ has a non-uniform distributed load pattern in the interface between the elastomer pad-liner and the bearing adapter. A maximum contact pressure of approximately 9,653 kPa (1400 psi) is present in the pressure test. The non-uniform distributed load pattern was further studied by changing the load to 60% of the full load.

Figure 7: Original Pressure Film Image with Load Pattern between the Elastomer Pad-Liner and the AdapterPlus™ at Full Load (~35,750 lbf)

Figure 8: 3D Image Load Pattern and Pressure Statistics at Interface between the Elastomer Pad-Liner and the AdapterPlus™ at Full Load (~35,750 lbf)

Figures 9 and 10 show the results of the pressure film tests for the load pattern and contact pressure at 60% of the full load between the elastomer pad-liner and the bearing adapter. These pressure film experiments show that the bearing AdapterPlus™ has a more pronounced non-uniform distributed load pattern in the interface between the elastomer

pad-liner and the bearing adapter (i.e. the load is mainly concentrated on the right and left sides of the elastomer pad-liner as shown in Figure 9). Thus, the load distribution is a function of the load applied to the pad. While at lower loads the pressure is concentrated on the sides, at higher loads the pressure becomes uniformly distributed.

Figure 9: Original Pressure Film Image with Load Pattern between the Elastomer Pad-Liner and the AdapterPlus™ at ~60% of Full Load

Statistics		
Image:	50%nostuds-lw010-02-12 Pseudocolor Rep	
Average	1,059.32	PSI
Std. Dev	404.23	PSI
Contact	20.93	sq.in
Total	40.65	sq.in
Force	22,174.6	lbf
Minimu	353.42	PSI
Maximu	1,400.00	PSI

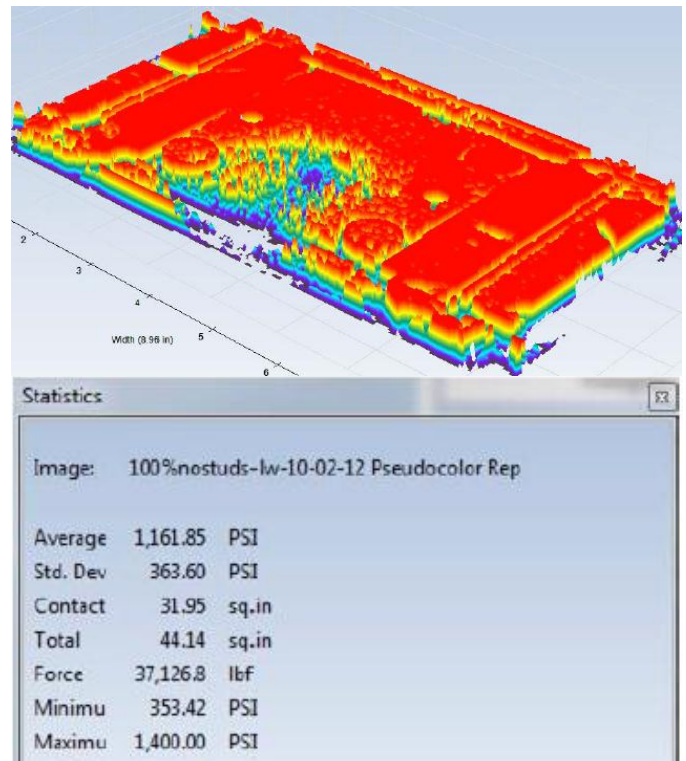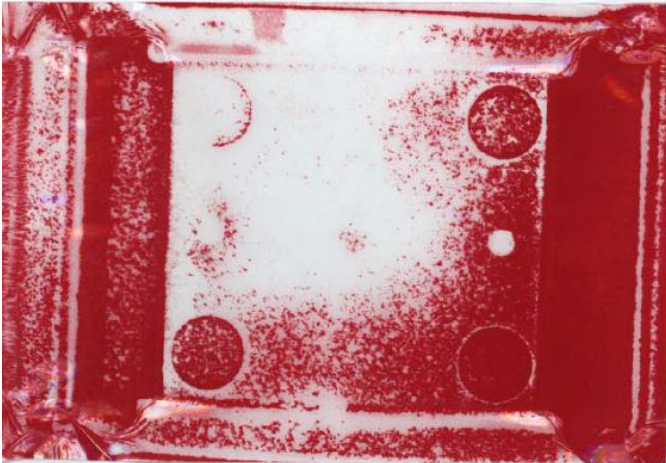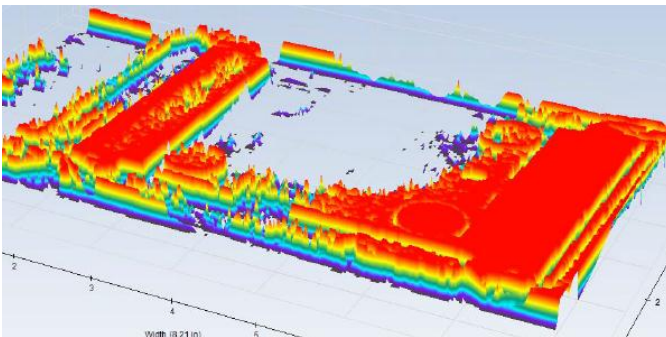**Figure 10: 3D Image Load Pattern and Pressure Statistics at Interface between the Elastomer Pad-Liner and the AdapterPlus™ at ~60% of Full Load**

STRESS ANALYSIS FINITE ELEMENT MODEL

The main objective of the work presented in this paper is to study the structural integrity of the modified bearing adapter during operation. FE models were created for two commonly used adapter types, namely, class K and class E bearing adapters.

Simplified CAD models for class E and class K adapters were constructed in Solid Works™. Figure 11 shows the CAD models for original & modified class E & class K Bearing Adapters. Ductile (nodular) iron with a density of $\rho=6.65\times10^{-4}$ lbf·s^2/in/in^3, a modulus of elasticity of $E=23\times10^6$ psi and a Poisson's ratio of $\upsilon=0.275$ was used for the bearing adapter material. As expected, reducing the modulus of elasticity does not change the stress distribution.
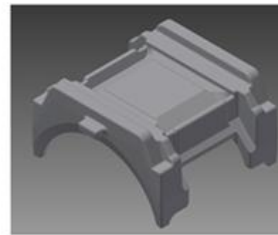
(a) Original Class E Bearing Adapter
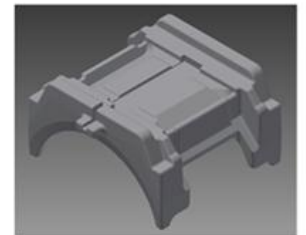
(b) Modified Class E Bearing Adapter
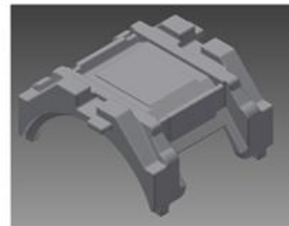
(c) Original Class K Bearing Adapter
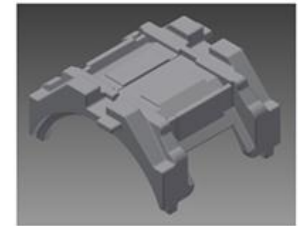
(d) Modified Class K Bearing Adapter

Figure 11: CAD Models for Original and Modified Class E & Class K Bearing Adapters

The CAD models were imported into ALGOR 20.3™, and discretized into approximately 300,000-800,000 elements with a mesh size of 0.075-0.21 in. for the adapter. A convergence analysis of the FE model revealed that the stress distribution results varied less than 10% when the mesh size was changed (see convergence section more details). A combination of bricks, wedges, pyramids and tetrahedral elements were used to successfully mesh the model. The brick and tetrahedral solid mesh provides an accurate mesh utilizing the fewest elements and allowing for a reduced analysis time. The differences between the numbers of elements depend on how the number of bricks and tetrahedral are distributed in each model and the volume of the different CAD models. In order to remove possible stress concentrations, a fillet was

introduced in the cutout of the modified adapters. Two different radii were used in order to see how the fillet will contribute to the stress distribution of the adapter and how it will affect our points of interest.

The distribution pattern of boundary conditions (pressure and pin constrains) for the FEM models were based on pressure film measurements. The pressure film results from between the bearing adapter and elastomer pad-liner were used in the FEM simulations by performing two cases. In case #1, the pressure distributes uniformly in the top surface; in case #2, the pressure doesn't distribute uniformly. A pressure at the top was obtained depending on the projected area of the applied load, and was then applied into the FEM simulations.

The results of the pressure film from between the bearing cup and bearing adapter were used in determining the bottom support of the adapter. It was found the bottom support was about four inches, which then was compared to two and six inch support in order to take into account variations in the manufactured parts.

As explained in the following sections, FEM models case #1 and case #2 show a uniform and non-uniform pressure at the top of the adapter at different supports of: two, four and six inches.

CASE # 1 FULL LOAD AND VARIABLE CONTACT BETWEEN THE BEARING CUP AND THE ADAPTER

As observed in the pressure film experiments, contact between the bearing cup and the adapter does not cover the full length of the raceways and it may fluctuate due to different tolerance factors. Values for the contact pressure of approximately four inches between the cup and adapter were obtained based on pressure film experiments (see experimental studies section). This contact length can significantly affect the stress distribution of the bearing adapter. Consequently, it is important to investigate if this contact length can be one of the major parameters that dictate the stress distribution in the bearing adapter.

The initial conditions studied for this case were that the raceways of the bearing adapter were supported by the bearing cup. Additionally, the raceways were supported by a pin constraint to simulate the support the bearing cup provides. A pressure equivalent to the full load on the projected surface was applied at the top. Figure 12 shows the bearing adapter assembly with colored flags marking the surfaces where specific boundary conditions were applied. Figure 12 and 13 show points of interest at the bottom center, top center, and cutout edges, used to compare results from different cases. Figure 14 shows a sample FEA result for class K modified adapter with full load and full raceway support.
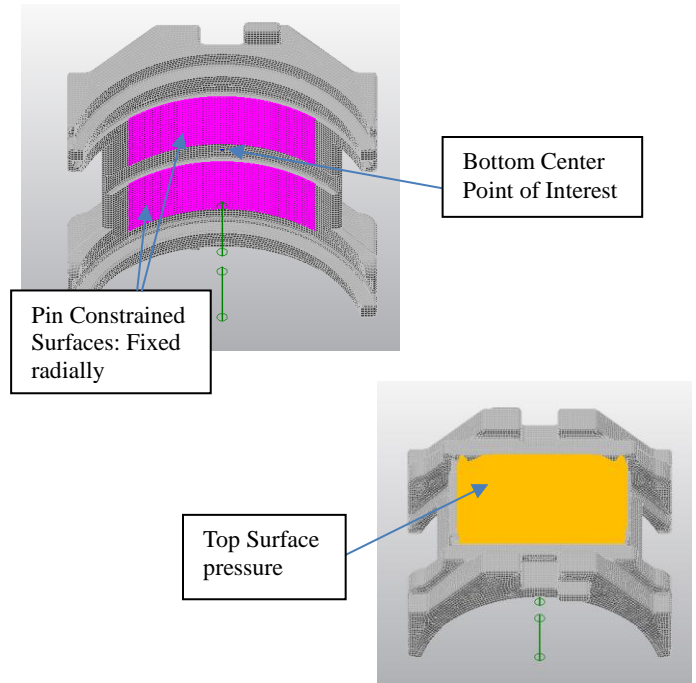

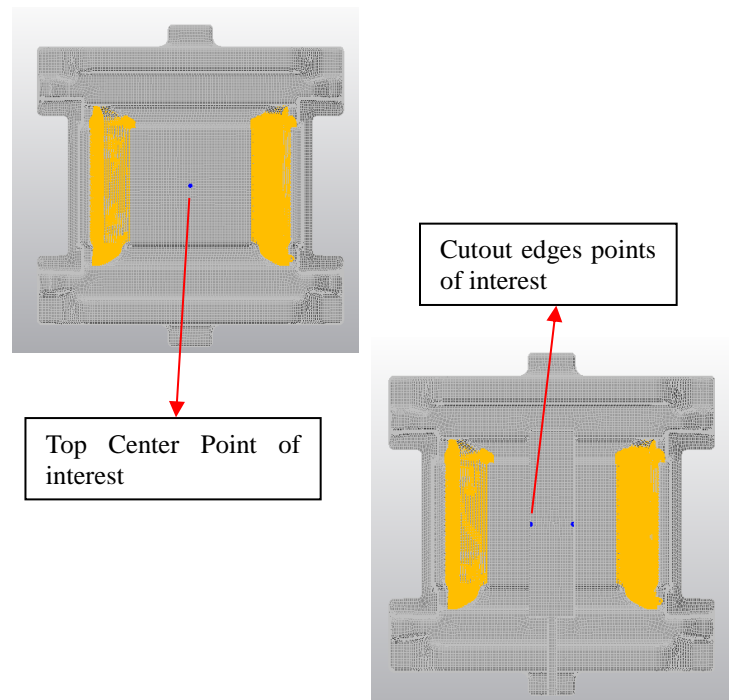**Figure 12: Case #1 Boundary Conditions on Finite Element Model and Points of Interest**

Figure 13: Class E Adapter Original and Modified Adapters with points of interest (Top View)
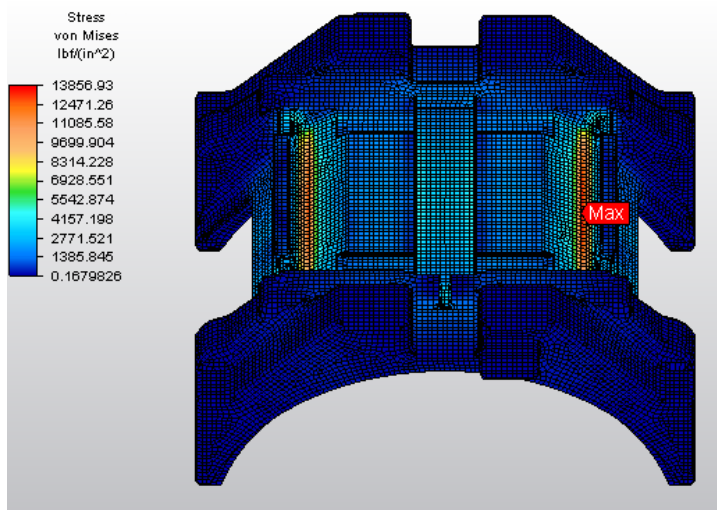
Figure 14: Sample FEA Result for Class K Modified Adapter with Uniformly Distributed Full Load and Six inch Raceway Support
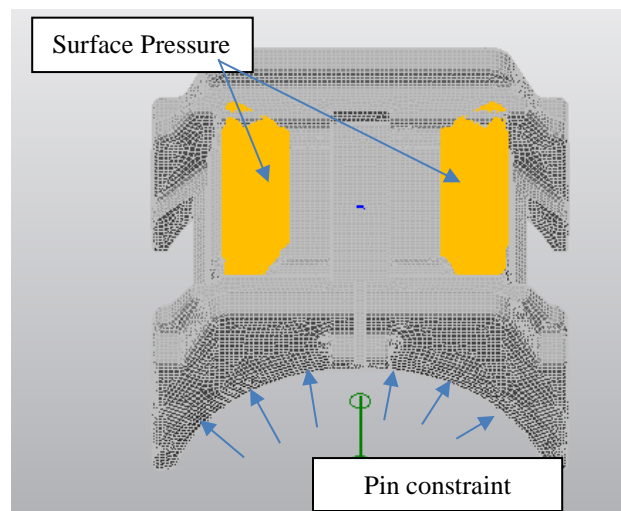
Figure 15: Case #2 Boundary Conditions on Finite Element Model

CASE # 2 FULL LOAD WITH NON-UNIFORM PRESSURE BETWEEN THE ELASTORMER PAD-LINER AND BEARING ADAPTER

Load distribution between the polymer pad-liner and the bearing adapter can also significantly affect the stress distribution of the bearing adapter. From the pressure film experiments, it was determined that loaded patterns range from a uniform pressure at the elastomer pad-liner and bearing adapter interface, to a non-uniform load distribution where the load concentrated on the left and right sides of the interface. Consequently, two different load distributions were studied to determine their impact on the stress distribution in the bearing adapter. Instead of a uniform load distribution, the load was distributed at the ends of the adapter based on pressure film experiments (see experimental studies section). Figure 15 shows the bearing adapter assembly with colored flags marking the surfaces where specific boundary conditions were applied. Figure 16 shows a sample FEA result for class E modified adapter with full load non-uniformly distributed and full raceway support.
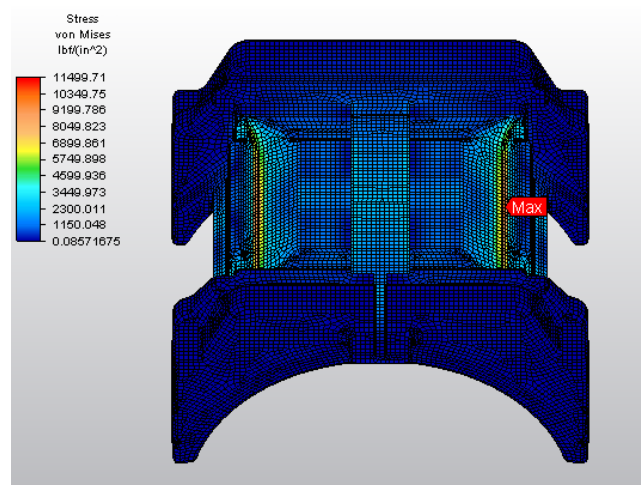
Figure 16: Sample FEA Result for Class E Modified Adapter with Non-Uniformly Distributed Full Load and 6 inch Raceway Support

FEA CONVERGENCE

The method used to show stress convergence and convergence to a reasonable level of accuracy is based on the literature [8]. The method for checking for convergence is to set three different level of model discretization (i.e. element size). The relationship between the three levels of model discretization (i.e. C-coarse, M-medium, and F-fine meshes) is shown in Table 1.

7

Table 1: Relationship between Coarse, Medium, and Fine Levels of Model Discretization

Mesh	1D	2D	3D
Coarse	N	N	N
Medium	λN	$λ^2$N	$λ^3$N
Fine	$λ^2$N	$λ^4$N	$λ^6$N

Where $λ$ is a scale factor and N is the number of elements. A convergence check can then be done with the following formula:

$$| σ_f − σ_m | / | σ_f | < \bar{e}_s$$

Where $σ_f$ and $σ_m$ are the stresses for the fine and medium meshes.

In practice, usually $\bar{e}_s$ less than 1% serves as an excellent level, and less than 10% as a satisfactory level. The results on this paper were checked using these criteria, and the results for each of the cases were found to be between 1-10%.

FEA RESULTS & INTERPRETATION

This section summarizes the FEA results for the two cases described in the previous section and provides an interpretation of the FEA results.

CASE # 1 VARIABLE CONTACT BETWEEN THE BEARING CUP AND THE ADAPTER

Table 2 and 3 summarize the FEA study results for class K original and modified adapters with uniform distributed load (i.e. full area pressure in the interface between the bearing adapter and the elastomer pad-liner) and variable contact between the bearing cup and adapter (e.g. contact length for two, four, and six inches respectively). The results include mesh size (in), number of elements, scale factor λ, Von Mises stresses at point of interest in the bottom center of the adapter, factor of safety at point of interest, convergence, and the maximum Von Mises stress in the FEA and its location. Von Mises stresses shown are unsmooth results from the analysis.

Table 2 shows that reducing contact length between the bearing cup and the adapter significantly increases Von Mises stresses. The increase of stresses appears to be non-linear. While the stresses increase by reducing the contact length from six inches to four inches, there is a more significant increase in stresses when the contact length was reduced to two inches. This is shown in Von Mises stresses at the point of interest (top surface) and the maximum stresses in the model. This is also observed in the maximum stresses for the modified adapter (refer Table 3). However, for the modified

adapter, it appears that removing material produced in some cases a redistribution of stresses around the point of interest. Comparing Tables 2 and 3, one finds that there is an increase of stresses (i.e. factor of safety decreases) due to the modifications of the adapter for onboard monitoring.

CASE # 2 FULL LOAD WITH NON-UNIFORM PRESSURE BETWEEN THE ELASTORMER PAD-LINER AND BEARING ADAPTER

Table 5 and 6 summarize the FEA study results for class K original and modified adapters with non-uniform distributed load (i.e. partial area pressure in the interface between the bearing adapter and the elastomer pad-liner) and variable contact between the bearing cup and adapter (e.g. contact length for two, four, and six inches respectively). The results also include mesh size (in), number of elements, scale factor λ, Von Mises stresses at point of interest in the bottom center of the adapter, factor of safety at point of interest, convergence, and the maximum Von Mises stress in the FEA and its location. Von Mises stresses shown are unsmooth results from the analysis.

Table 5 shows that the non-uniform distributed load between the elastomer pad-liner and the bearing adapter significantly increases Von Mises stresses particularly at lower contact lengths. The increase of stresses seems to be non-linear. This is shown in Von Mises stresses at the point of interest and the maximum stresses in the model. This is also observed in the maximum stresses for the modified adapter (refer Table 5). However, for the modified adapter, it appears again that removing material produced in some cases a redistribution of stresses around the point of interest. Comparing Table 5 and 6, one finds that there is an increase of stresses (i.e. factor of safety decreases) due to the modifications of the adapter for onboard monitoring.

While the non-uniform pressure between the elastomer pad-liner and bearing adapter shows large effect on stresses, it is important to recall that pressure films experiments showed that higher loads tend to produce uniform pressures at this interface. The significance of the obtained results is the realization that even load that are a fraction of full load may produce very significant stresses if there is a non-uniform pressure developed in the elastomer pad-liner and bearing adapter interface.

FULL LOAD WITH UNIFORM AND NON-UNIFORM PRESSURE BETWEEN THE ELASTORMER PAD-LINER AND BEARING ADAPTER (CLASS E)

Table 8, 9 and 10 show the results for the class E original and modified adapter with a uniform distributed load; while Table 11, 12 and 13 show the results for the class E original and modified adapters with a non-uniform distributed load. Similarly to previous results, the points of interest that were

recorded in these FEA studies were a point at the center top for the original adapter or the top edges of the cutout for the modified adapter.

As in previous results it can be seen that the Factor of Safety decreases as the bottom support decreases. The maximum stresses are located at the imposed boundary conditions. The class E original adapter has a volume of 84.12 sq. in. while the modified adapter has a volume of 82.8 sq. in. This accounts for a 1.57% reduction in volume.

Table 2: Results for Class K Original Adapter with Uniform Distributed Load

Contact Length	Mesh	Mesh Size (in)	Number of Elements	λ	VM Stress on top (psi)	FS	Convergence	Max VM Stress (psi)	Location
2 inch	Medium	0.2	94,190	1.69	6,328.45	6.32	7.05%	94,727	Edge of raceway
	Fine	0.1	456,745		6,808.17	5.88			
4 inch	Medium	0.2	91,988	1.71	2,346.46	17.05	0.99%	24,715	Edge of raceway
	Fine	0.1	456,225		2,370.04	16.88			
6 inch	Medium	0.2	95,823	1.56	2,476.06	16.15	1.38%	10,165	Edge of raceway
	Fine	0.11	361,191		2,,510.75	15.93			

Table 3: Results for Class K Modified Adapter (0.05 in fillet) with Uniform Distributed Load

Contact Length	Mesh	Mesh Size (in)	Number of Elements	λ	VM Stress on cutout edge (psi)	FS	Convergence	Max VM Stress (psi)	Location
2 inch	Medium	0.2	95,067	1.50	18,835.68	2.12	7.07%	90,468	Edge of raceway
	Fine	0.1	322,025		17,592.06	2.27			
4 inch	Medium	0.2	91,144	1.52	4,076.94	9.81	3.12%	27,153	Edge of raceway
	Fine	0.1	317,294		3,953.55	10.12			
6 inch	Medium	0.2	92,845	1.52	3,203.98	12.48	1.65%	7,881	Edge of raceway
	Fine	0.1	324,862		3,257.59	12.28			

Table 4: Results for Class K Modified Adapter (0.1 in fillet) with Uniform Distributed Load

Contact Length	Mesh	Mesh Size (in)	Number of Elements	λ	VM Stress on cutout edge (psi)	FS	Convergence	Max VM Stress (psi)	Location
2 inch	Medium	0.2	93,293	1.52	13,073.00	3.06	5.98%	65,406	Edge of raceway
	Fine	0.1	326,758		13,905.09	2.88			
4 inch	Medium	0.195	99,422	1.50	3,294.47	12.14	8.87%	19,188	Edge of raceway
	Fine	0.1	336,388		3,615.28	11.06			
6 inch	Medium	0.2	90,959	1.54	3,135.28	12.76	7.18%	7,894	Edge of raceway
	Fine	0.1	330,712		3,377.78	11.84			

Table 5: Results for Class K Original Adapter with Non-Uniform Distributed Load

Contact Length	Mesh	Mesh Size (in)	Number of Elements	λ	VM Stress on top (psi)	FS	Convergence	Max VM Stress (psi)	Location
2 inch	Medium	0.2	94,190	1.69	11,491.84	3.48	2.99%	167,312	Edge of raceway
	Fine	0.1	456,745		11,158.17	3.58			
4 inch	Medium	0.2	91,988	1.71	2,393.01	16.72	0.55%	48,196	Edge of raceway
	Fine	0.1	456,225		2,379.81	16.81			
6 inch	Medium	0.2	95,823	1.56	2,715.01	14.73	1.64%	20,199	Top Surface
	Fine	0.11	361,191		2,760.35	14.49			

Table 6: Results for Class K Modified Adapter (0.05 in fillet) with Non-Uniform Distributed Load

Contact Length	Mesh	Mesh Size (in)	Number of Elements	λ	VM Stress on cutout edge (psi)	FS	Convergence	Max VM Stress (psi)	Location
2 inch	Medium	0.2	95,067	1.50	39,488.25	1.01	8.02%	157,628	Edge of raceway
	Fine	0.1	322,025		36,556.27	1.09			
4 inch	Medium	0.2	91,144	1.52	6,639.84	6.02	1.76%	69,625	Edge of raceway
	Fine	1	317,294		6,524.94	6.13			
6 inch	Medium	0.2	86,519	1.55	4,640.68	8.62	0.67%	14,729	Top Surface
	Fine	0.11	324,862		4,671.91	8.56			

Table 7: Results for Class K Modified Adapter (0.1 in fillet) with Non-Uniform Distributed Load

Contact Length	Mesh	Mesh Size (in)	Number of Elements	λ	VM Stress on cutout edge (psi)	FS	Convergence	Max VM Stress (psi)	Location
2 inch	Medium	0.2	93,293	1.52	9,267.67	4.32	5.90%	40,730	Edge of raceway
	Fine	0.1	326,758		9,848.33	4.06			
4 inch	Medium	0.21	86,637	1.57	5,035.84	7.94	1.74%	37,859	Edge of raceway
	Fine	0.1	336,388		4,949.75	8.08			
6 inch	Medium	0.2	90,959	1.54	4,349.42	9.20	7.91%	13,748	Top Surface
	Fine	0.1	330,712		4,723.10	8.47			

Table 8: Results for Class E Original Adapter with Uniform Distributed Load

Contact Length	Mesh	Mesh Size (in)	Number of Elements	λ	VM Stress on top (psi)	FS	Convergence	Max VM Stress (psi)	Location
2 inch	Medium	0.145	144,351	1.64	4,381.77	9.13	5.49%	34,459	Edge of Raceway
	Fine	0.073	639,486		4,636.38	8.63		50,258	
4 inch	Medium	0.14	170,113	1.62	2,583.97	15.48	3.92%	10,831	Edge of Raceway
	Fine	0.075	721,557		2,689.49	14.87		15,503.7	
6 inch	Medium	0.14	125,013	1.78	2,676.45	14.95	3.90%	8,446	Edge of Raceway
	Fine	0.075	704,967		2,785.14	14.36		10,662	

Table 9: Results for Class E Modified Adapter (0.05 in fillet) with Uniform Distributed Load

Contact Length	Mesh	Mesh Size (in)	Number of Elements	λ	VM Stress on cutout edge (psi)	FS	Convergence	Max VM Stress (psi)	Location
2 inch	Medium	0.12	181,457	1.58	8,398.81	4.76	7.36%	42,107	Edge of Raceway
	Fine	0.075	720,886		9,017.21	4.44		58,274	
4 inch	Medium	0.12	191,106	1.58	3,383.10	11.82	2.82%	13,479	Edge of Raceway
	Fine	0.075	748,361		3,478.61	11.50		15,250	
6 inch	Medium	0.125	177,533	1.67	3,227.92	12.39	1.18%	10,272	Edge of Raceway
	Fine	0.074	829,550		3,189.80	12.54		11,492	

Table 10: Results for Class E Modified Adapter (0.1 in fillet) with Uniform Distributed Load

Contact Length	Mesh	Mesh Size (in)	Number of Elements	λ	VM Stress on cutout edge (psi)	FS	Convergence	Max VM Stress (psi)	Location
2 inch	Medium	0.12	208,648	1.55	7,341.235	5.45	8.24%	42,686	Edge of Raceway
	Fine	0.074	783,158		7,946.28	5.03		54,655	
4 inch	Medium	0.12	209,190	1.56	3,188.435	12.55	5.10%	13,433	Edge of Raceway
	Fine	0.074	794,831		3,351.025	11.94		16,371	
6 inch	Medium	0.12	220,622	1.52	3,114.365	12.84	6.49%	9,438	Edge of Raceway
	Fine	0.075	774,749		3,316.6	12.06		10,689	

Table 11: Results for Class E Original Adapter with Non-Uniform Distributed Load

Contact Length	Mesh	Mesh Size (in)	Number of Elements	λ	VM Stress on top (psi)	FS	Convergence	Max VM Stress (psi)	Location
2 inch	Medium	0.145	144,351	1.64	5,939.73	6.73	5.15%	41,454	Edge of Raceway
	Fine	0.075	639,486		6,262.01	6.39		61,679	
4 inch	Medium	0.145	170,113	1.62	1,825.81	21.91	1.08%	21,400	Edge of Raceway
	Fine	0.075	721,557		1,845.75	21.67		29,818	
6 inch	Medium	0.14	125,013	1.78	1,939.26	20.63	1.74%	13,452	Top Surface
	Fine	0.075	704,967		1,973.59	20.27			

Table 12: Results for Class E Modified Adapter (0.05 in fillet) with Non-Uniform Distributed Load

Contact Length	Mesh	Mesh Size (in)	Number of Elements	λ	VM Stress on cutout edge (psi)	FS	Convergence	Max VM Stress (psi)	Location
2 inch	Medium	0.12	181,457	1.58	13,026.22	3.07	8.25%	53,762	Edge of Raceway
	Fine	0.075	720,866		14,100.37	2.84		75,152	
4 inch	Medium	0.12	191,106	1.58	3,449.05	11.60	1.52%	27,009	Edge of Raceway
	Fine	0.075	748,361		3,501.31	11.42		30,283	
6 inch	Medium	0.11	177,533	1.67	2,864.705	13.96	2.03%	14,442	Top Surface
	Fine	0.074	829,550		2,806.69	14.25		15,541	

Table 13: Results for Class E Modified Adapter (0.1 in fillet) with Non-Uniform Distributed Load

Contact Length	Mesh	Mesh Size (in)	Number of Elements	λ	VM Stress on cutout edge (psi)	FS	Convergence	Max VM Stress (psi)	Location
2 inch	Medium	0.12	208,648	1.55	10,933.60	3.66	9.77%	54,260	Edge of Raceway
	Fine	0.074	783,158		12,001.96	3.33		70,004	
4 inch	Medium	0.12	209,190	1.56	2,859.76	13.99	7.49%	26,806	Edge of Raceway
	Fine	0.074	794,831		3,073.90	13.01		32,477	
6 inch	Medium	0.12	220,622	1.52	2,557.25	15.64	6.79%	15,027	Top Surface
	Fine	0.075	774,749		2,730.84	14.65		16,191	

CONCLUSIONS

Understanding the structural integrity of modified bearing adapters during operation is essential. This paper begins to quantify the reliability of the bearing adapter through a series of finite element analyses and pressure film experiments. Different sensitivity analyses were performed to study the dependence of the results on boundary conditions and material properties.

The finite element and experimental results show that there is an increase of stresses (i.e. factor of safety decreases) due to the modifications of the adapter for onboard monitoring. The increase of stresses, which may be significant, is a function of different parameters including the interface properties between the bearing adapter and the elastomer pad-liner and the bearing adapter and cup. The pressure film experiments show that the interface properties are a function of the load. Specifically, this study quantified the changes in the stress distribution in the bearing adapter based on the pressure loads

between the bearing cup and the adapter and between the elastomer pad-liner and the bearing adapter.

While the non-uniform pressure between the elastomer pad-liner and bearing adapter and the small contact length between the bearing cup and adapter show large effects on stresses, it is important to recall that pressure film experiments showed that higher loads tend to produce uniform pressures. It is also expected that higher loads will tend to increase the contact length between the bearing cup and the adapter. The significance of the obtained results also includes the realization that even loads that are a fraction of full load may produce very significant stresses if there is a non-uniform pressure developed in the elastomer pad-liner and bearing adapter interface which will impact the life of the bearing adapter.

Additional work is being conducted to complete the structural integrity study of conventional and modified railroad bearing adapter for onboard monitoring. Ongoing work includes additional experiments to validate the finite element model using instrumented adapters and additional case studies including the case of dynamic loading under worst case scenarios (e.g. flat wheel). Finally, the information from experiments and FEA studies is being used to estimate the lifetime of original and modified railroad bearing adapters under different service conditions.

NOMENCLATURE

CL Contact Length between Bearing Cup and Adapter (in)
FS Factor of Safety
λ Scale factor
VM Von Mises

ACKNOWLEDGMENTS

REFERENCES

[1] Karunakaran, S., Snyder, T.W., *Bearing Temperature Performance in Freight Cars*. in *ASME RTD 2007 Fall Technical Conference*. 2007. Chicago, Illinois.

[2] Vernersson, T., *Temperatures at Railway Tread Braking. Part 1: Modeling.* Proceedings of the Institution of Mechanical Engineers: Journal of Rail and Rapid Transit, 2007. 221 part F(2): p. 167-182.

[3] Sukumaran Nair, V.P., Prabhakaran Nair, K., *Finite element analysis of elastohydrodynamic circular journal bearing with micropolar lubricants.* Finite Elements in Analysis & Design, 2004. 41(1): p. 75-89.

[4] Wang, H., *Axle Burn-Off and Stack-Up Force Analyses of a Railroad Roller Bearing Using the Finite Element Method*, 1996, University of Illinois at Urbana-Champaign, Urbana, IL.

[5] Dunnuck, D.L., *Steady-State Temperature and Stack-Up Force Distributions in a Railroad Roller Bearing Assembly*, 1992, University of Illinois at Urbana-Champaign, Urbana, IL.

[6] Saenz IV, L., *Calibration and Optimization of a Load Sensor Embedded in a Railroad Bearing*, 2012, Master of Science Thesis, Department of Mechanical Engineering, The University of Texas-Pan American.

[7] Zagouris, A., Fuentes, A.A., Tarawneh, C.M., Kypuros, J.A., Arguelles, A., Experimentally Validated Finite Element Analysis of Railroad Bearing Adapter Operating Temperatures, Proceedings of the ASME 2012 International Mechanical Engineering Congress and Exposition, November 9-15, Houston, Texas.

[8] Sinclair, G. B., *Practical Convergence-Divergence Checks for Stresses from FEA,* 2006, *Proceedings of the 2006 International ANSYS Conference*, Pittsburgh, PA.